Performances of Laser Plasma Accelerators

Victor Malka, J. Faure, C. Rechatin, A. Ben Ismail, J. Lim

Laboratoire d'Optique Appliquée, ENSTA-Ecole Polytechnique, CNRS, 91761 Palaiseau, France

E. Lefebvre, X. Davoine
CEA/DAM Ile-de-France, France

CERN, CARE annual meeting, Decembre 02-05 (2008)

Partially supported by CARE-Euroleap-Accel1 contracts

LOA

Development of compact magnets

B=0.41 T

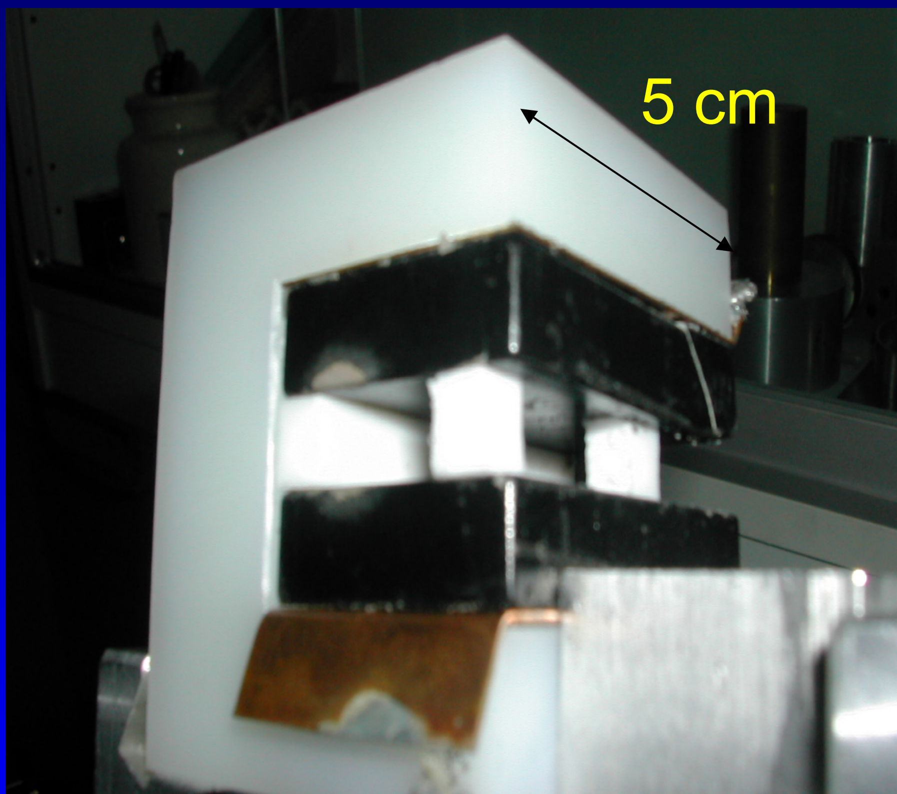

Previous Magnet
home made, up to 100 MeV

B=1 T

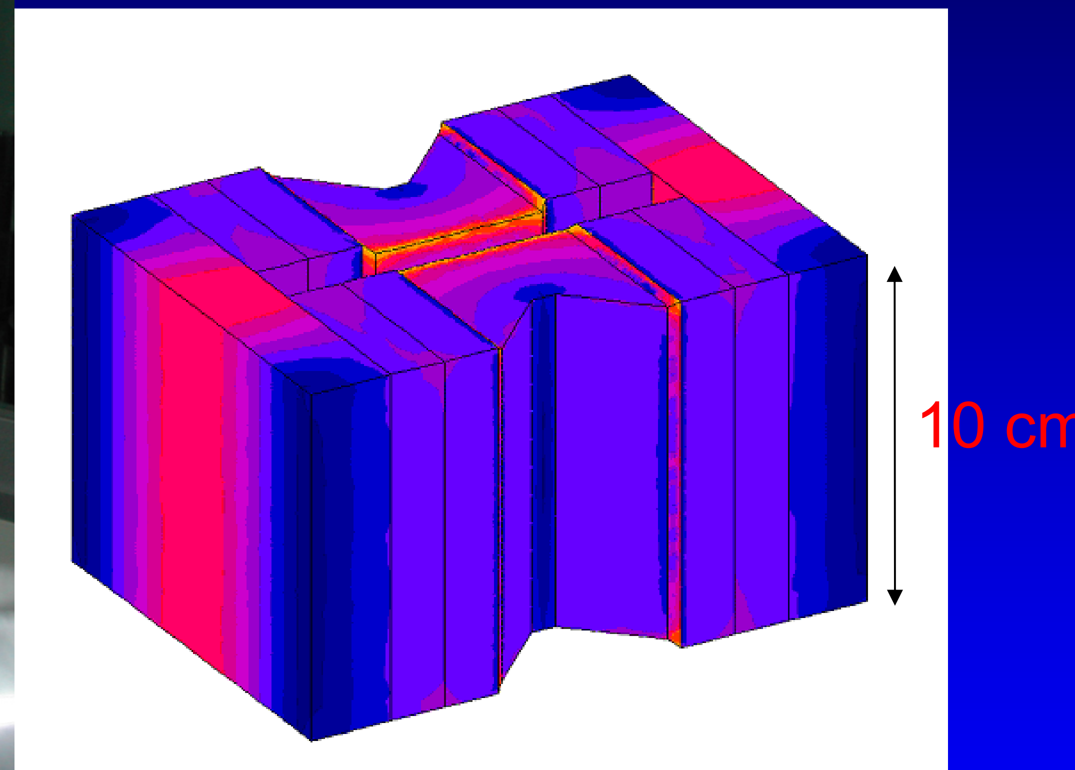

Design of a new magnet
up to 400 MeV

Data from the manufacturer

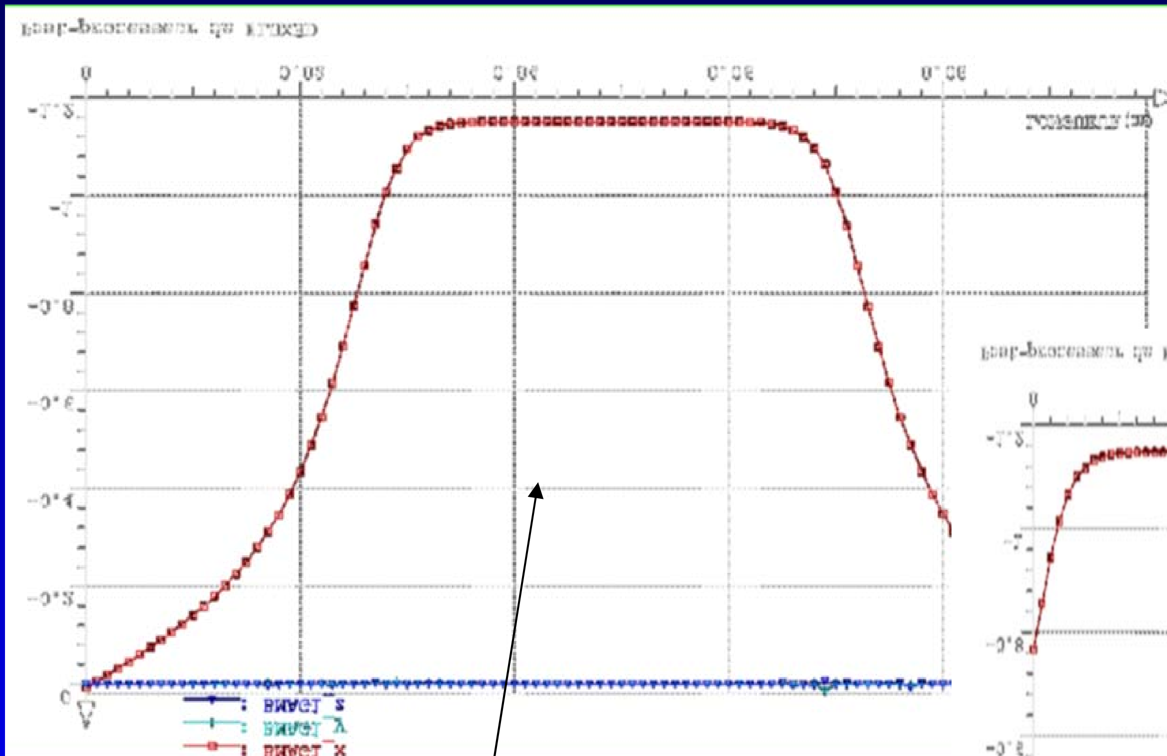

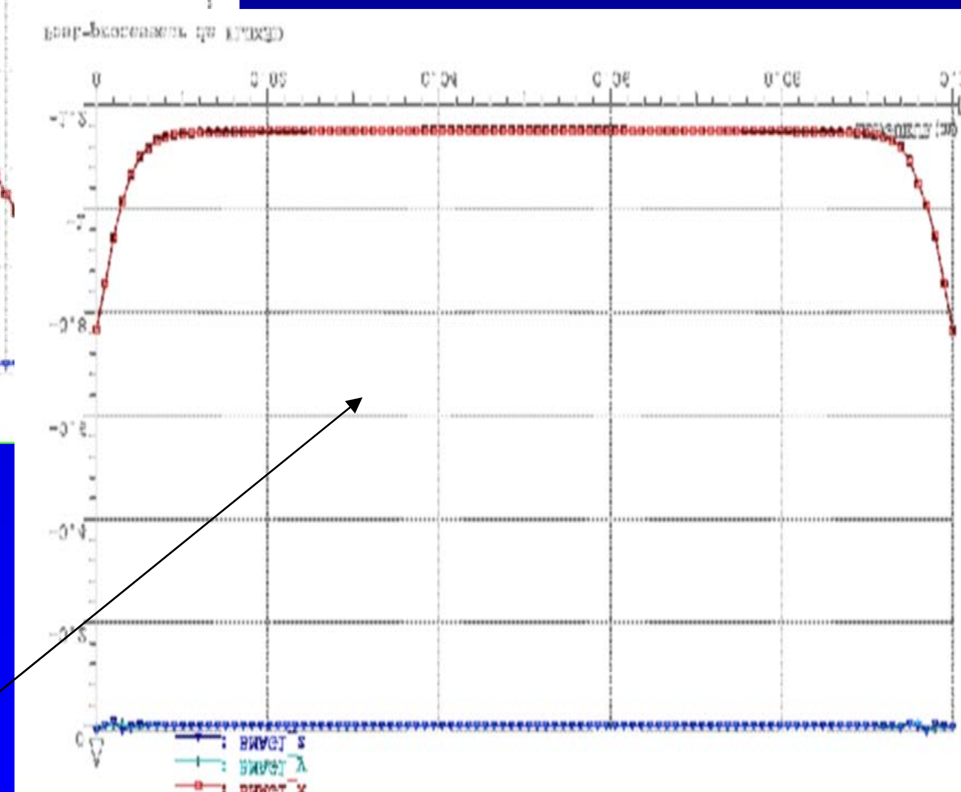

Simulations of the longitudinal magnetic field

Transverse magnetic field

L O A

Experimental setup

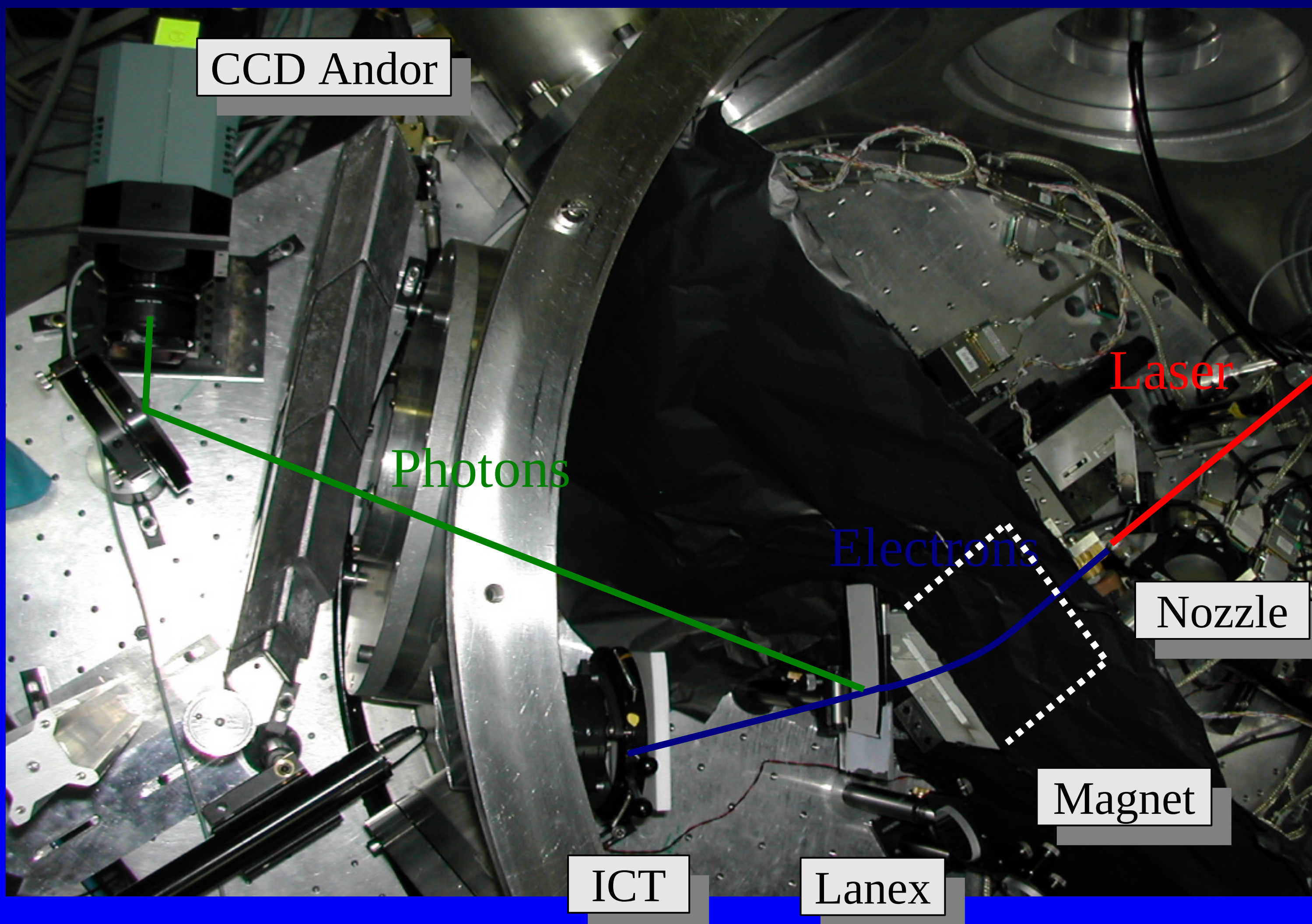

L O A

POLYTECHNIQUE

ENSTA

Analytical calculations

- Trajectories of an electron in a permanent magnetic field
  - Radius of curvature (relativistic electron):

$$R = E_0/B_m ec$$

E_0 Initial kinetic energy
B_m Magnetic field
e Charge of the electron
c Celerity of light

- Assumptions :
  - The magnetic field is uniform in a rectangular area
  - The relativistic incomming electron is perpendicular to the magnet's surface.

Coordinates

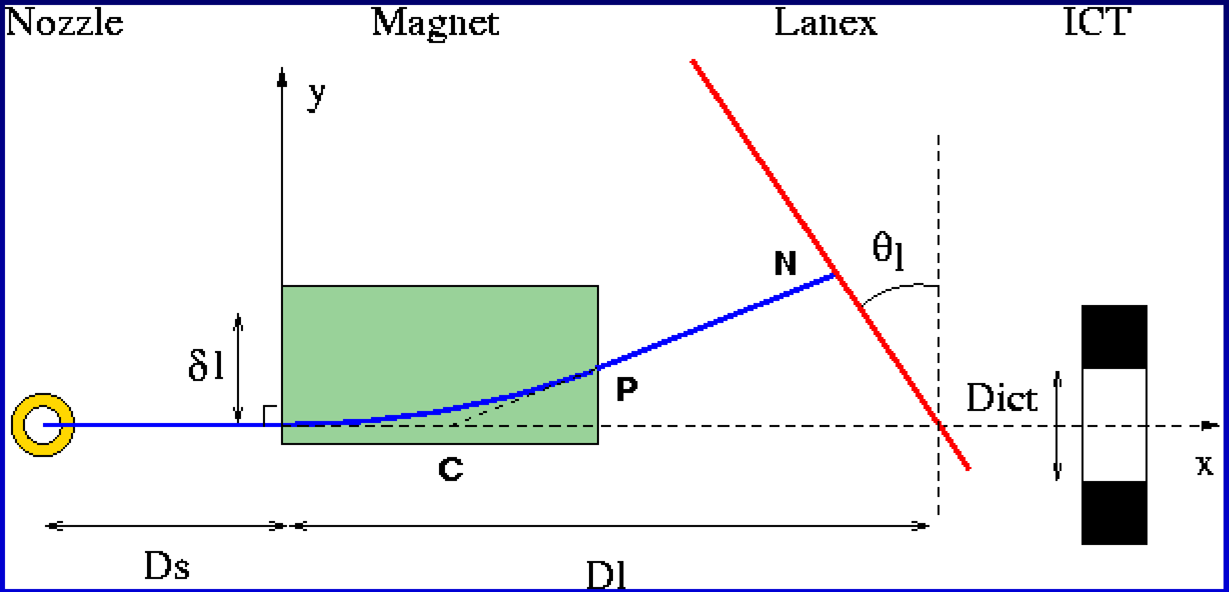

$$\begin{pmatrix} x_P \\ y_P \end{pmatrix} = \begin{pmatrix} L_m \\ R - \sqrt{R^2 - L_m^2} \end{pmatrix}$$

$$\begin{pmatrix} x_C \\ y_C \end{pmatrix} = \begin{pmatrix} \dfrac{x_P^2 + y_P^2}{2\, x_P} \\ 0 \end{pmatrix}$$

$$\begin{pmatrix} x_N \\ y_N \end{pmatrix} = \begin{pmatrix} D_l - y_l \tan(\theta_l) \\ \dfrac{(D_l - x_C)\, y_P}{x_P - x_C + y_P \tan(\theta_l)} \end{pmatrix}$$

Equivalent magnetic field

- The real magnetic field spreads outside the magnet. The introduction of an equivalent magnetic field allows the use of analytical formulas.

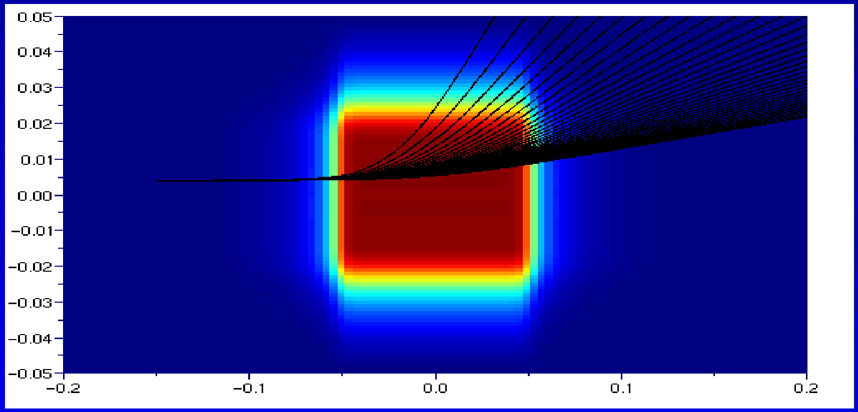

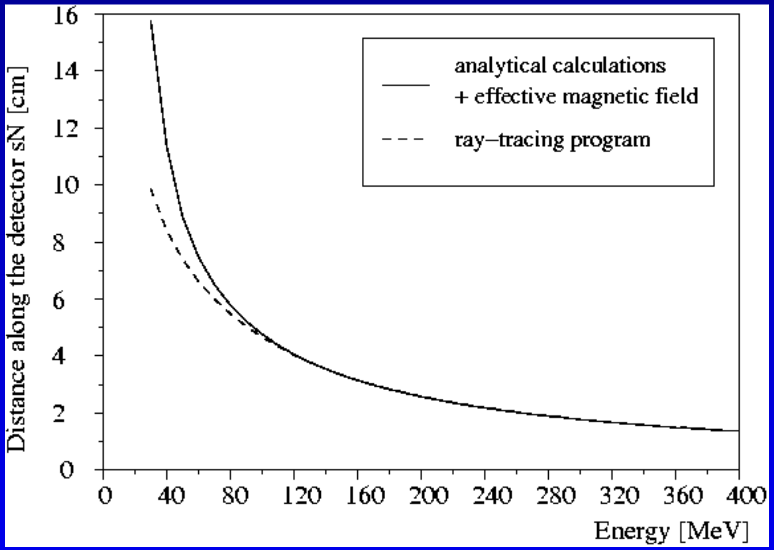

- Not valid for electrons below 100 MeV who travel in the gradient of the magnetic field

LOA

Detector composition

Item	Material	Density (g/cc)	Thickness (cm)
Laser Shielding			
Shielding	Aluminium	2,70	0,0100
Kodak Lanex Fine Screen			
protective coating	cellulose acetate	1,32	0,0010
plastic subtrate	Poly(ethylene terephtalate)	1,38	0,0178
scintillator	Gd2O2S + urethane binder	4,25	0,0084
protective coating	cellulose acetate	1,32	0,0005

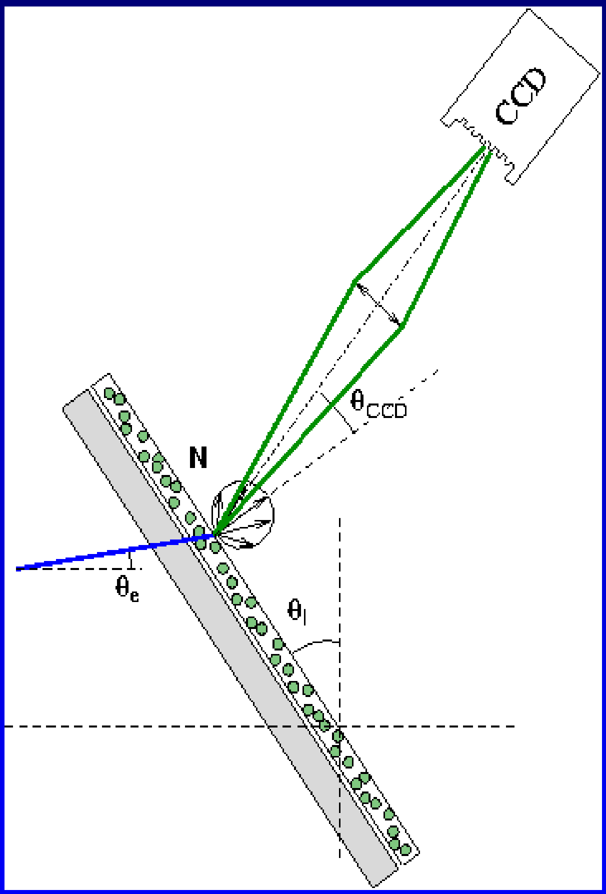

Composition of the scintillating screen

The surface loading of Gadolinium Oxysulfide in the urethane binder is 33 mg/cm^2

Schach von Wittenau *et al.*, Med. Phys. **29** pp. 2559-2570 (2002)

Absolute calibration

Phosphor layer : conversion

We assume that the conversion into visible light is proportional to the energy deposited in the scintillator layer

$$\frac{dN_{cr}}{dN_{el}} = \frac{1}{E_{ph}} \varepsilon \frac{dE}{dx} \delta x$$

$\delta x = h_S / \rho_{GOS}$ effective phosphor thickness

ε efficiency

Transport : photon collection

The transmission at the phosphor boundary and the number of photons collected by the lens of the Andor CCD

$$\frac{dN_{coll}}{dN_{cr}} = \zeta\, g(\theta_{CCD})\, \delta\Omega\, q_l\, q_Q\, q_{IF}$$

ζ output transmission factor

$g(\theta_{CCD})$ lambertian law

Detection by the CCD : number of counts

The yield of the Andor CCD camera

$$\frac{dN_{count}}{dN_{coll}} = \frac{QE}{r}$$

$$\frac{dN_{el}}{dE} dE = Counts \div \left(\frac{dN_{counts}}{dN_{coll}} \frac{dN_{coll}}{dN_{cr}} \frac{dN_{cr}}{dN_{el}} \right)$$

L O A

List of parameters

Parameter	Symbol	Value
Spectrometer		
Magnet		
Equivalent magnetic field	Bm	0.41 T
Magnet length	Lm	5 cm
Magnet width	Lm	2.5 cm
Magnet shift	dm	1.3 cm
Magnet-Lanex length	Dl	17 cm
Lanex		
Lanex angle	ql	55°
Efficiency	e	0.16
Surface Loading	hs	33 mg/cm2
Phosphor density	rGOS	7.44 g/cm3
Photon energy	Eph	2.27 eV
Transmission factor	z	0,22
ICT		
ICT diameter	Dict	10 cm

Parameter	Symbol	Value
Detection System		
Solid Angle	dW	2.0e-3 sr
CCD angle	qccd	15°
Lens	ql	0,95
Quartz	qq	0,95
Interference filter	qIF	0,2
Pixel size on the lanex	dxpix	0.28 mm
Electron Source		
Source-Magnet length	Ds	6 cm
Divergence	qs	10 mrad

From absolute calibration at ELYSE

L O A

ENSTA POLYTECHNIQUE CNRS

Comparison

- Charge estimated for the same images using the ICT and the absolute calibration of the Lanex
  - Bias of the ICT (ratio not constant)
  - More sensitivity of the Lanex film at low density
- Possible origin of this high value :
  - Sensitivity to the electro-magnetic signal from the interaction
  - Sensitivity to the huge amount of low-energy electrons which are not seen on the scintillator.
  - Unknown effect for electrons which flow inside the spires or in the vicinity of the ICT.
- No observation of direct saturation of the scintillator.
- Absolute calibration gives a local information.

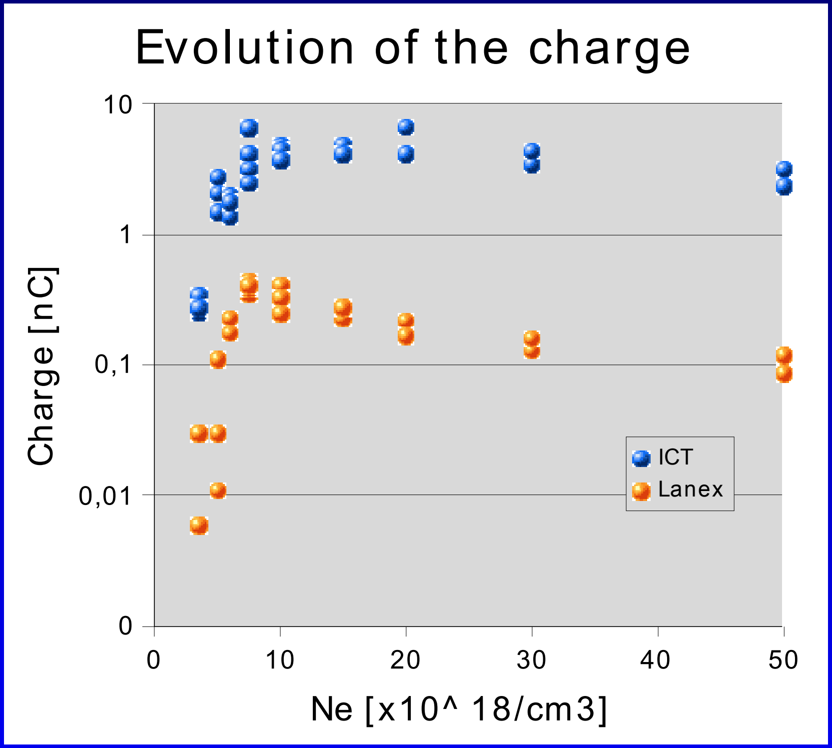

L O A

Absolute calibration of the LANEX KODAK FINE

- Calibration of the scintillator response on a RF accelerator
  - ELYSE : a laser-triggered picosecond electron accelerator

Linearity with charge

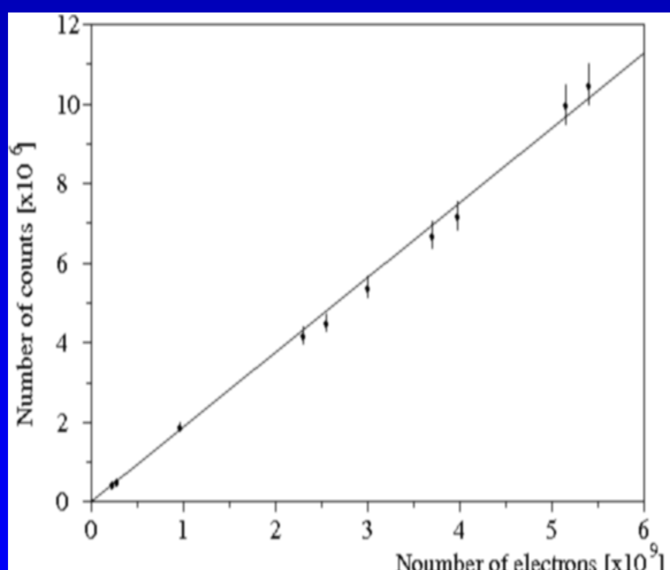

Independence of the yield with electron energy

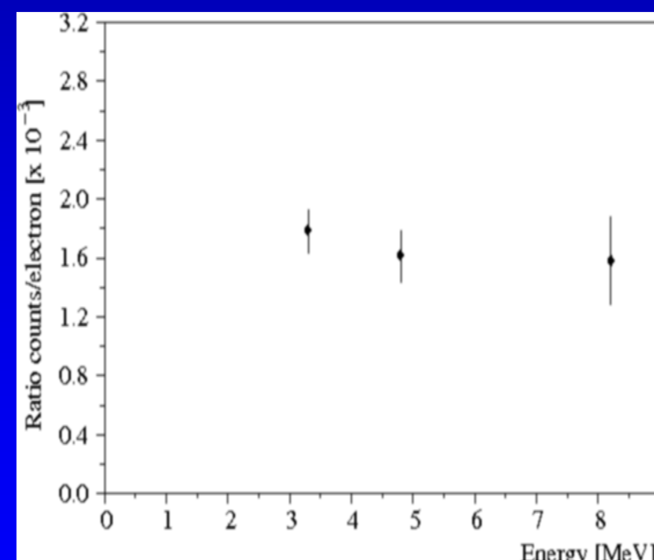

Previously checked for Imaging Plate (Fuji BAS-SR2025) : Tanaka *et al*., Rev. Sci. Instr. (2005)

Extension for laser-plasma interaction

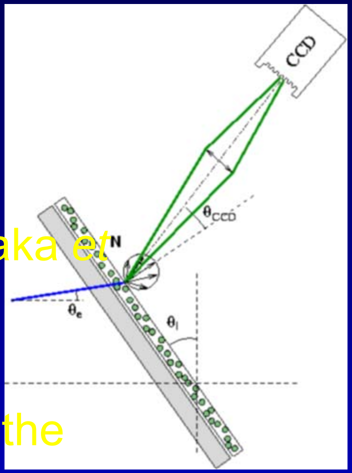

- Global yield of the detection system
  - Intrinsic yield of pure GOS : independent of the electron energy (Tanaka *et al*, Rev. Sci. Instr. 2005)
  - Transmission factor at the interface and output light distribution
  - Collection angle of the lens and conversion into number of counts on the CCD chip.

- Assumption that the scintillator efficiency remains constant
  - Retrieve the intrinsic conversion efficiency of this scintillator (fraction of energy deposited in pure GOS layer which is converted into visible light)

    e ~ 16 %
  - Close to the value for X-rays (in the range 15-20 %) : Giakoumakis *et al*, Phys. Med. Biol. (1989)
  - Can be used in other configurations

Glinec *et al*, accepted in RSI

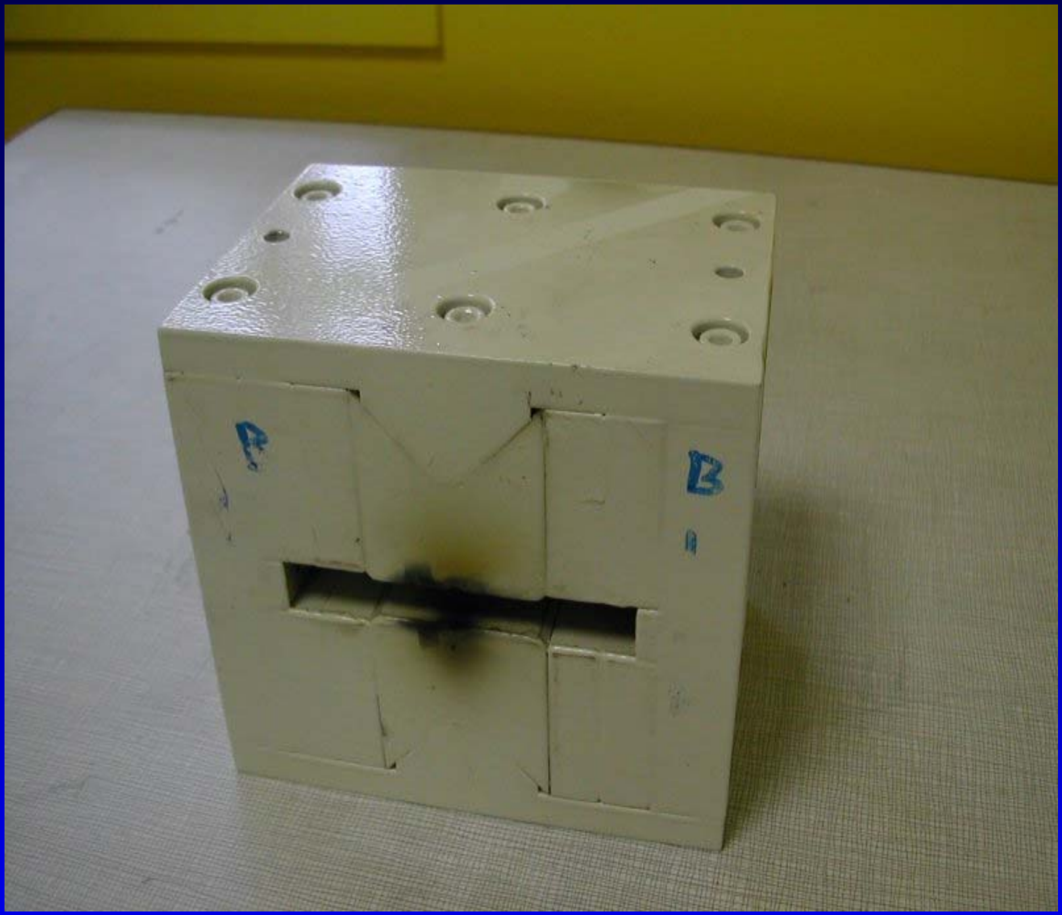

10 cm magnet

40 cm new magnet for GeV e beam

L O A

ENSTA

POLYTECHNIQUE

CNRS

From SMLFW to Bubble :
From Mono to maxwellian spectra

Electron density scan

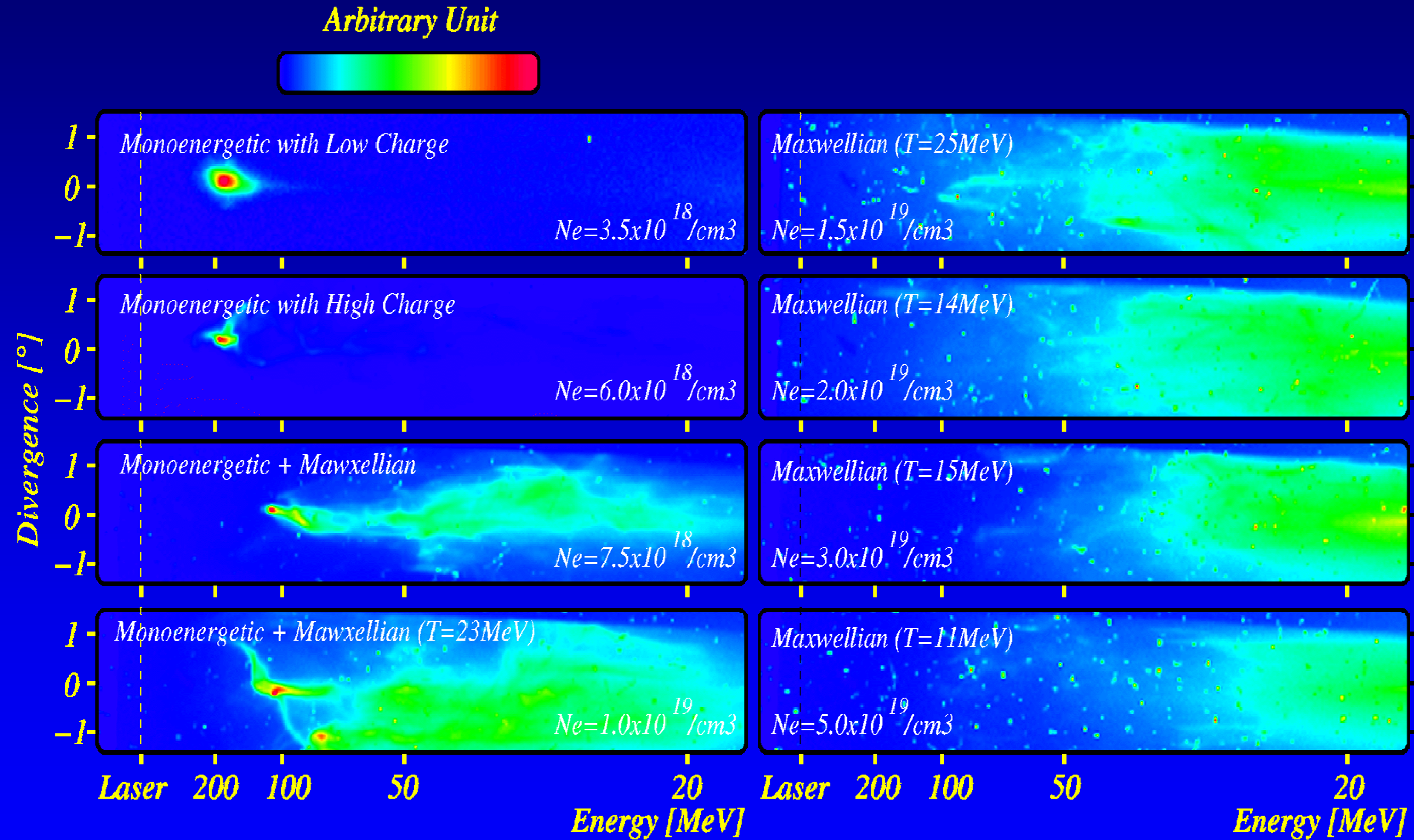

V. Malka *et al.*, **PoP** 2005

L O A

ENSTA

POLYTECHNIQUE

CNRS

Energy distribution improvements: The Bubble regime

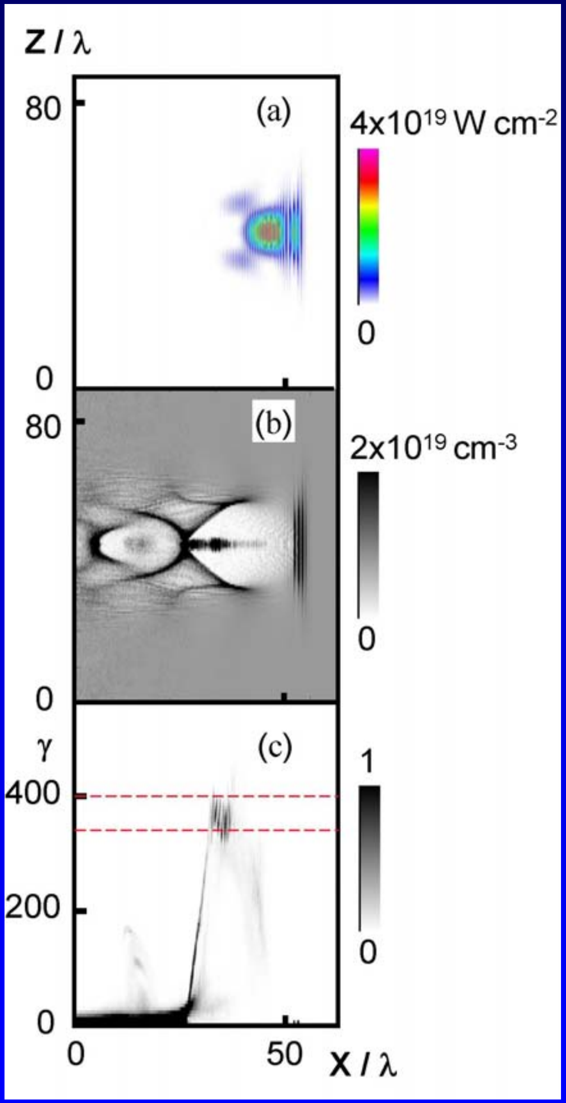

Charge in the peak : 200-300 pC

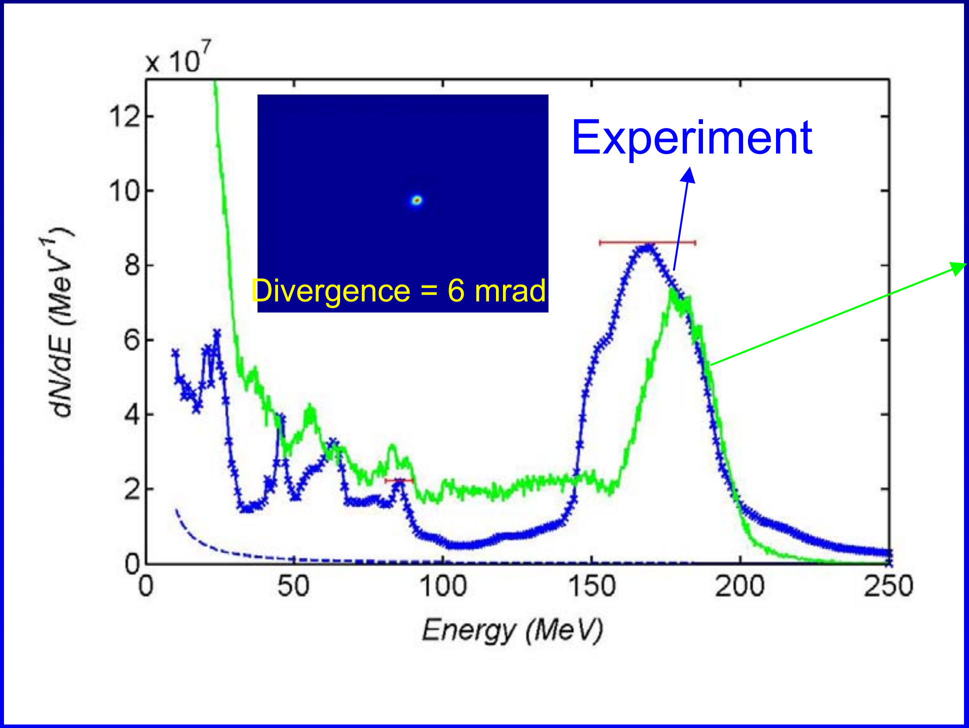

At LOA

J. Faure *et al.*, **Nature** (2004)

LOA

Controlling the injection

A second laser beam is used to heat electrons

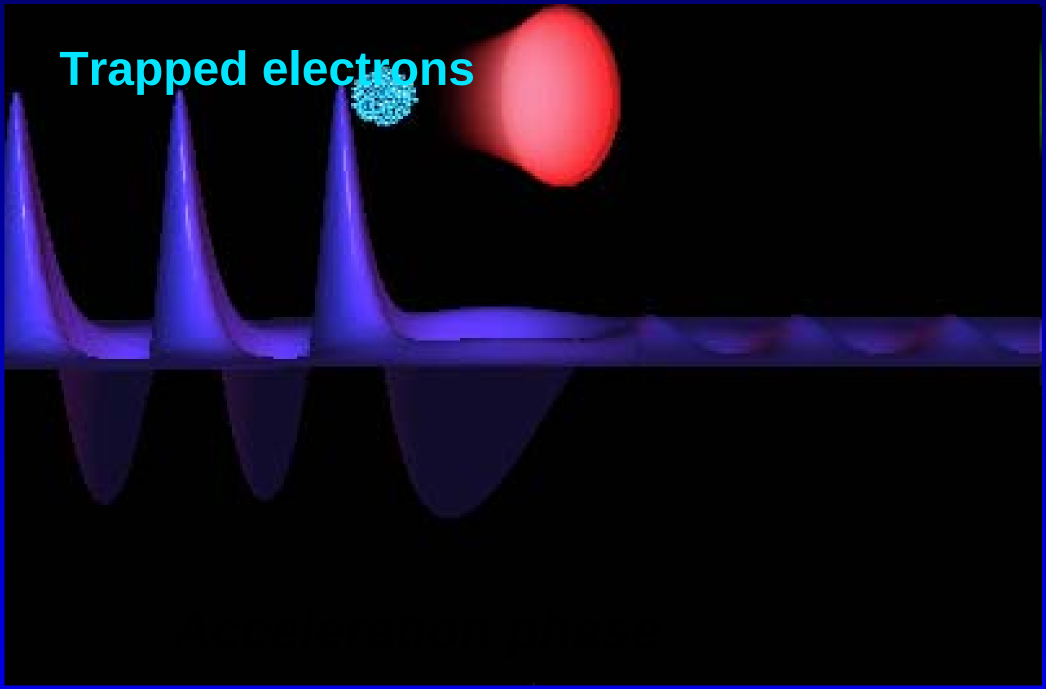

Ponderomotive force of beatwave: $F_p \sim 2a_0a_1/\lambda_0$ (a_0 et a_1 can be "weak")

Boost electrons locally and injects them

INJECTION IS LOCAL and IN FIRST BUCKET

E. Esarey *et al.*, **PRL** 79, 2682 (1997), G. Fubiani *et al.* (**PRE** 2004)

L O A

Experimental set up

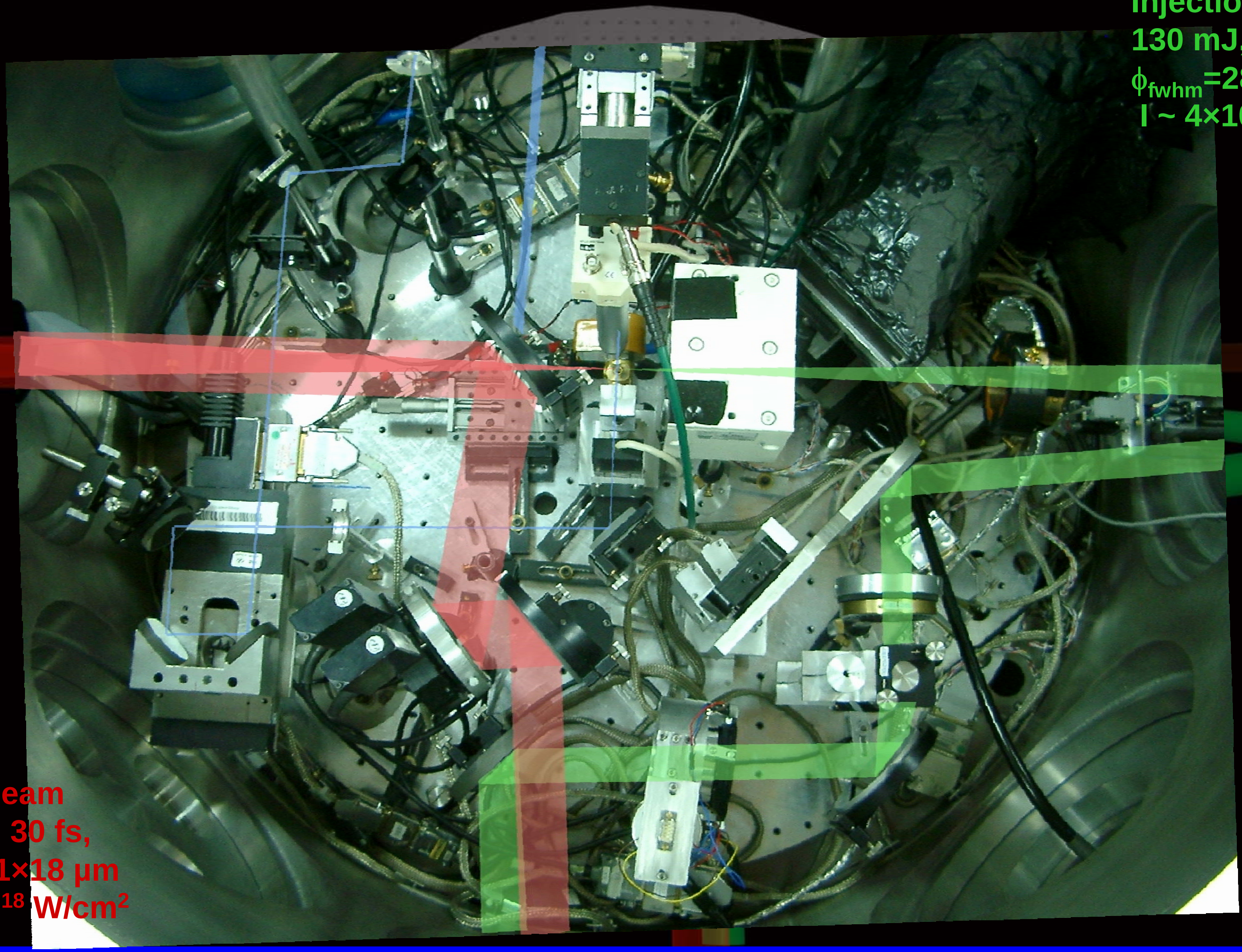

Injection beam
130 mJ, 30 fs
ϕ_{fwhm}=28× 23 µm
I ~ 4×10^{17} W/cm^{2}

Pump beam
670 mJ, 30 fs,
ϕ_{fwhm}=21×18 µm
I ~ 4×10^{18} W/cm^{2}

L O A

Tunable monoenergetic bunches

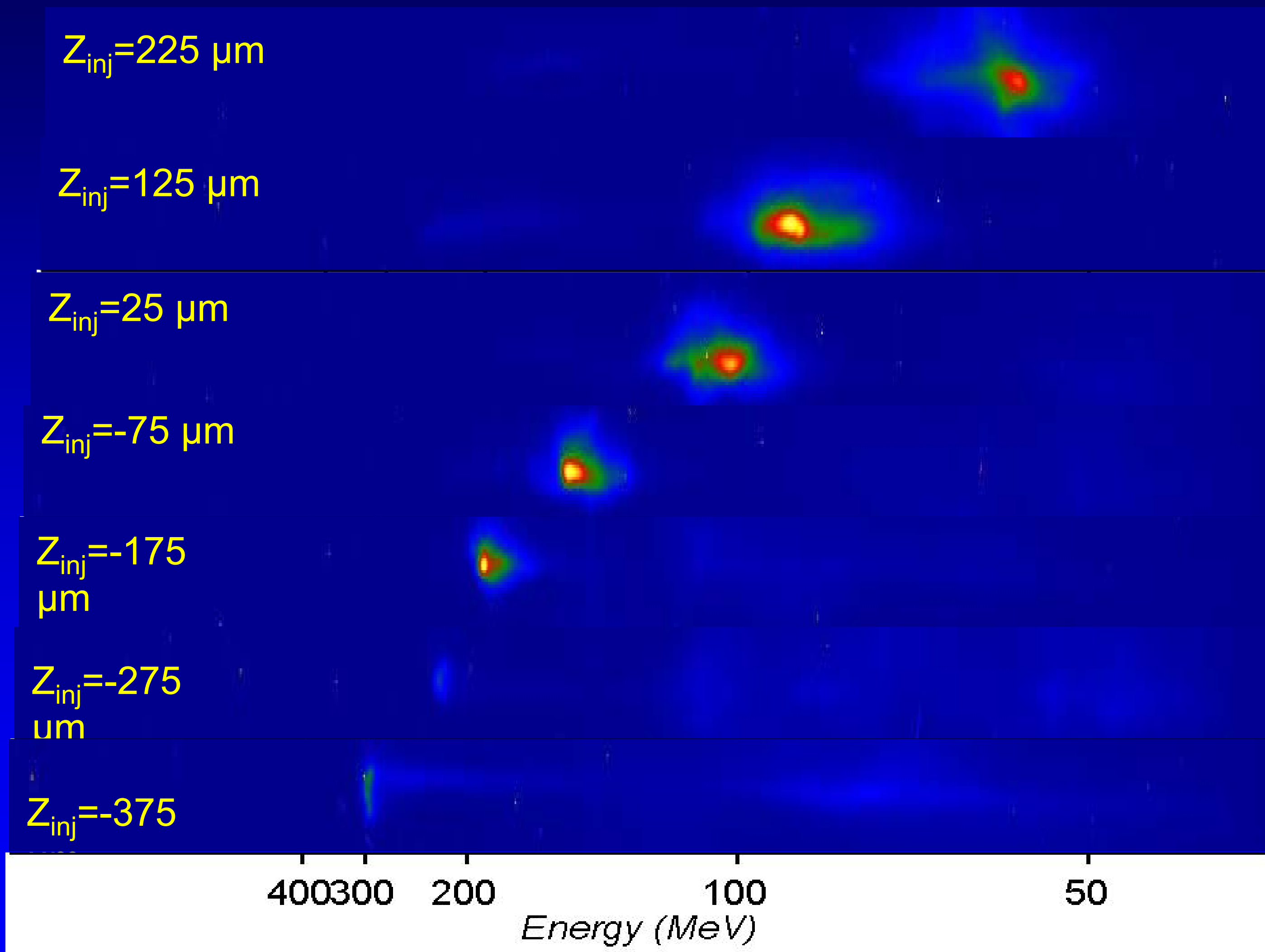

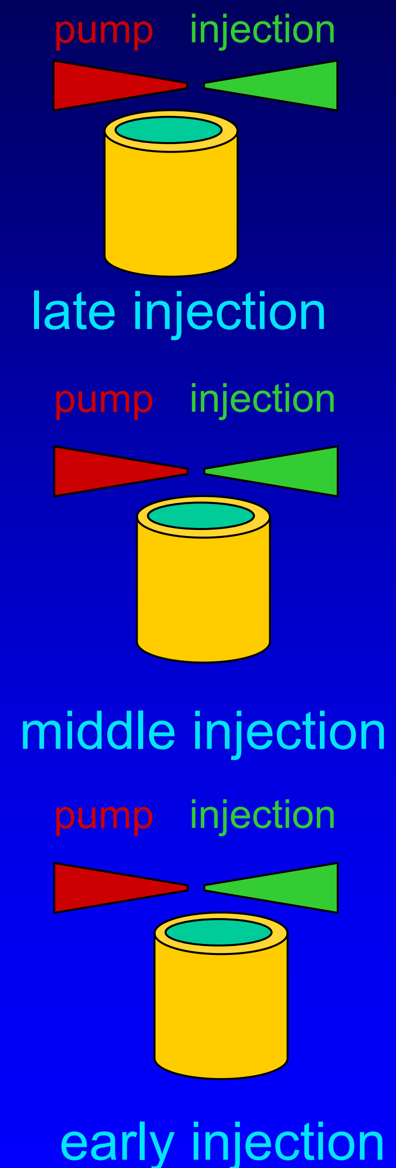

J. Faure *et al.*, **Nature 2006**

Non collinear geometry

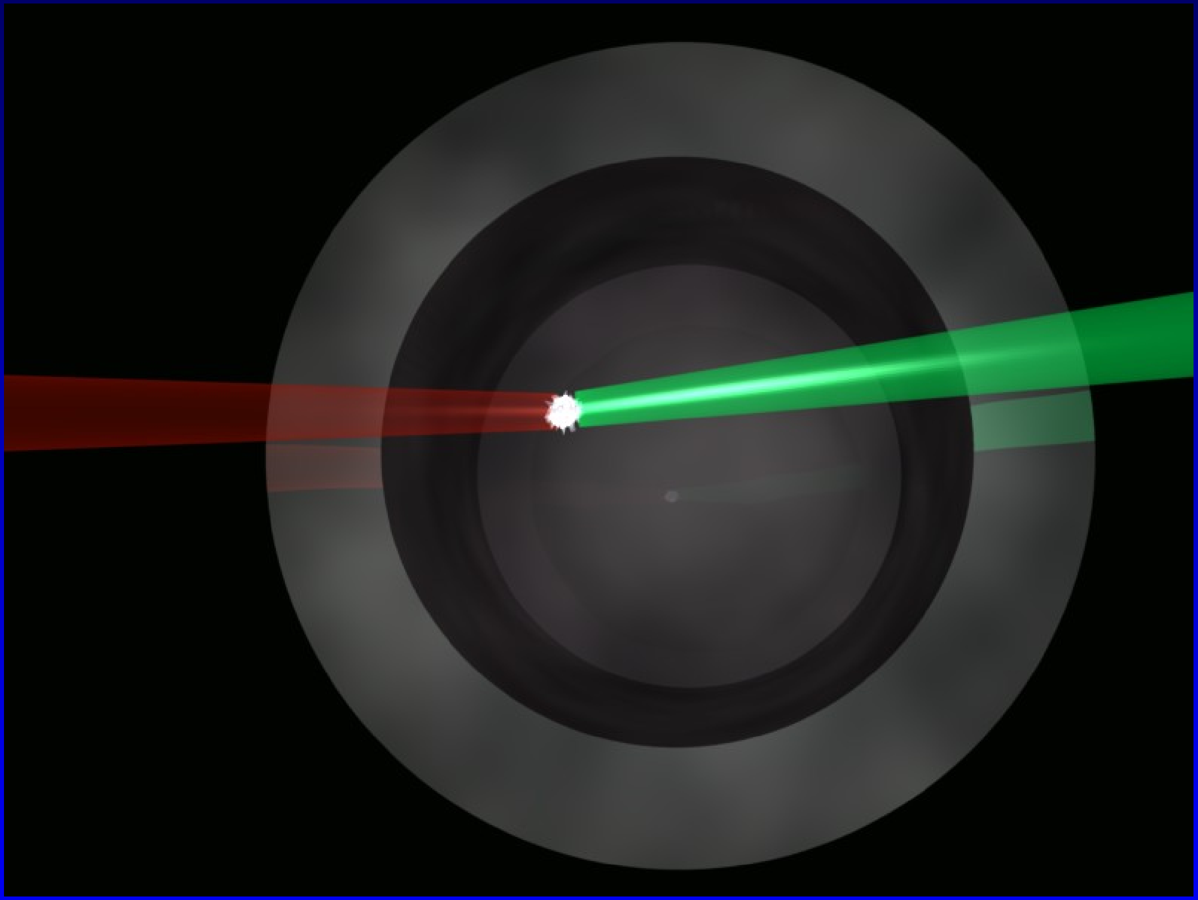

Advantages

- No feedback (2 mJ of light scattered from the plasma)
- Easier access to use e-beams for applications or diagnostics

Drawbacks

- Synchronization is more critical
- Tuning the energy is more difficult

θ=4.5°

Focal spots are about 25 µm FWHM. Beam overlap occurs over $L=(w_0+ w_1)/\tan(\theta)$

L ~ 600-1000 µm : not that critical + tuning still possible

L O A

Stable monoenergetic beams at 200 MeV

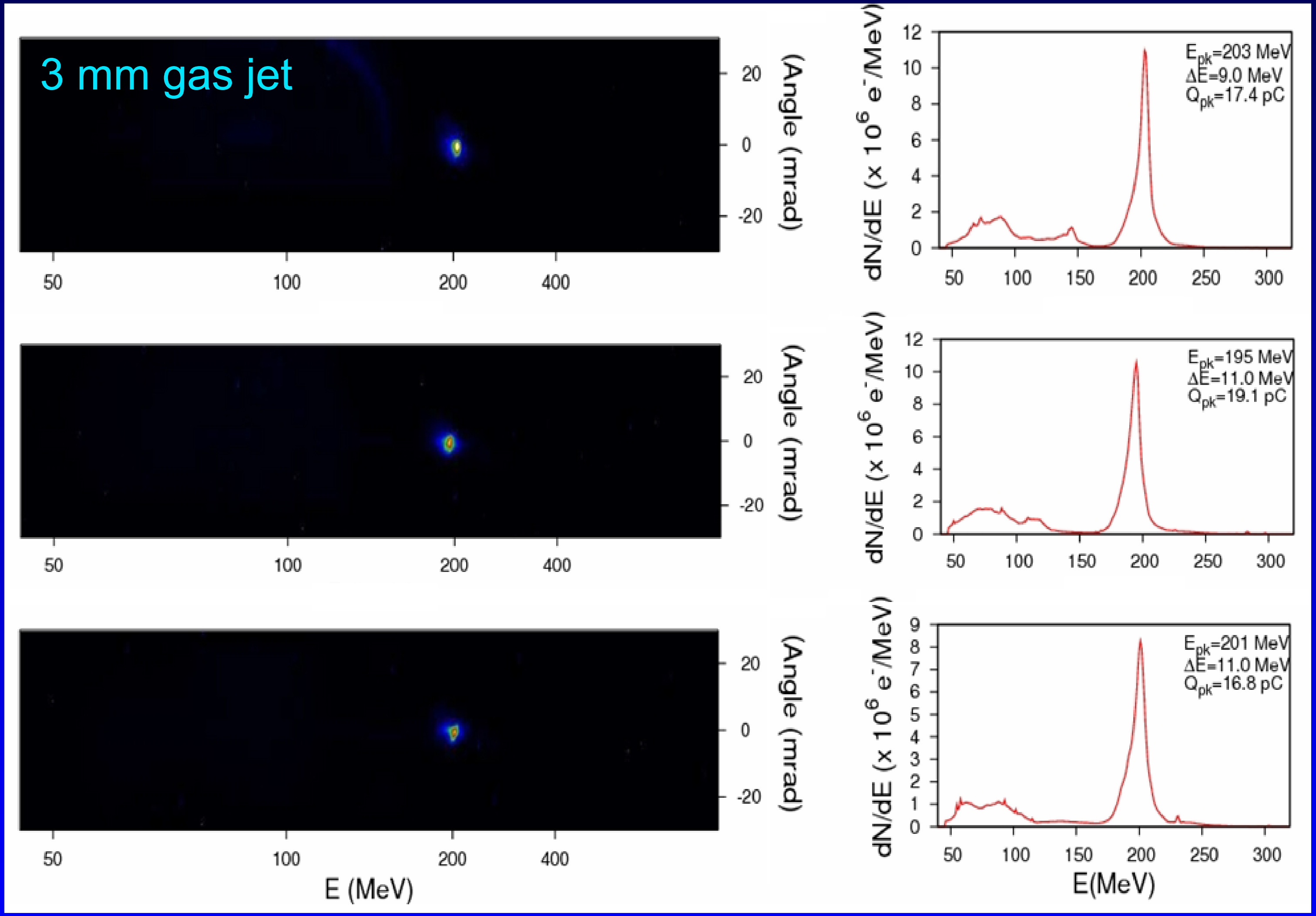

Statistics (30 shots):

E = 206 +/- 11 MeV

Qpk = 16.5+/- 4.7 pC

δE = 14 +/- 3 MeV

δE/E = 6%

Very little electrons at low energy
δE/E=5% limited by spectrometer

L O A

Energy tuning in non-collinear geometry

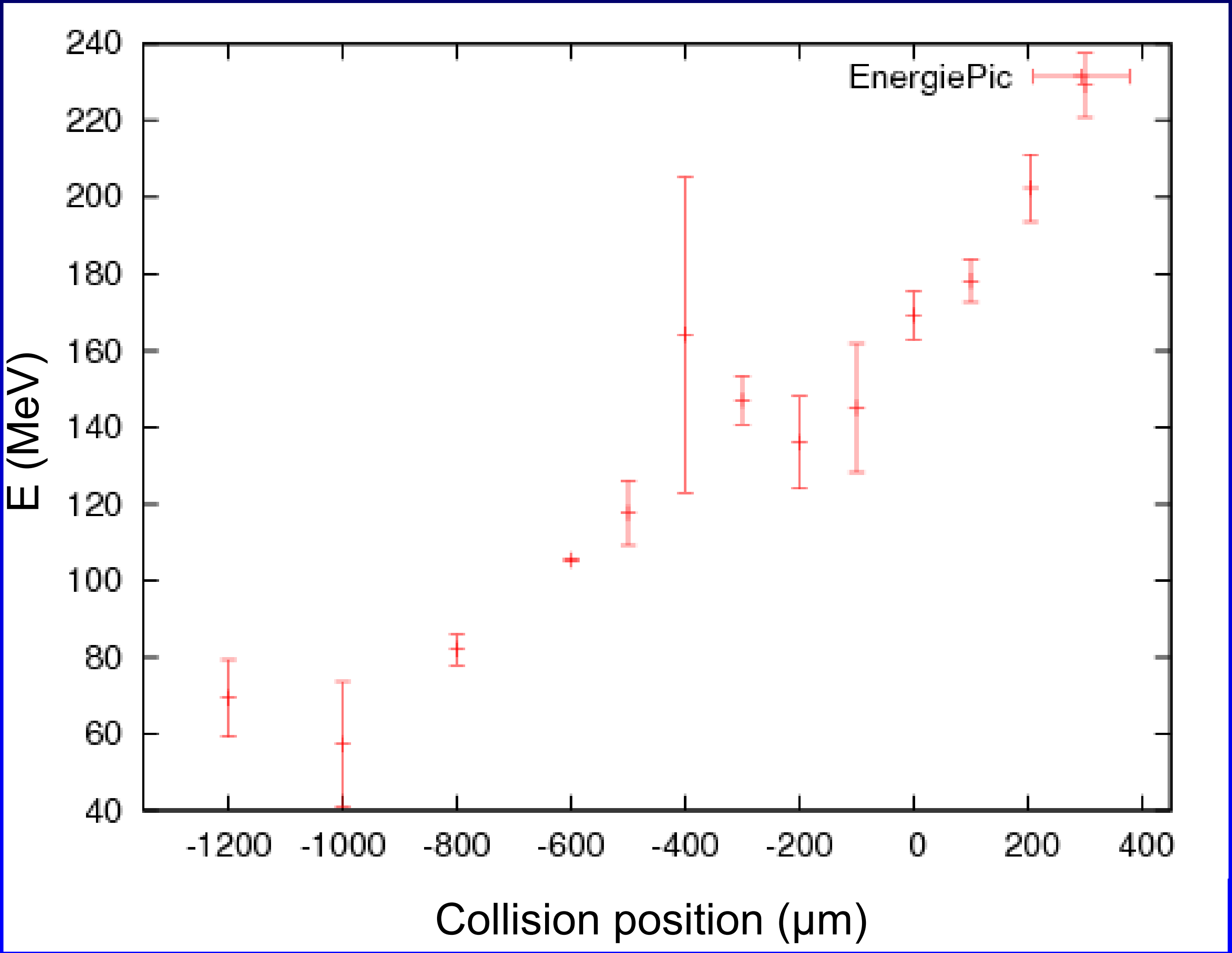

L O A

Tuning the charge and the energy spread

- **Charge can be tuned by**

  Controlling Heating electrons processes

  →Changing intensity of injection beam: smaller a_1 means less heating and less trapping

- **Energy spread can be tuned by**

  Decreasing the phase space volume V_{trap} of trapped electrons

  Changing the ratio V_{trap}/λ_p^3 by changing n_e (by changes λ_p^3) or a_1 (changes V_{trap})

In practice, energy spread and charge are correlated:
Decreasing a_1 decreases the charge but also V_{trap}, and in consequence the energy spread

Tuning the energy spread with the plasma density

2 mm gas jet

Increasing pressure

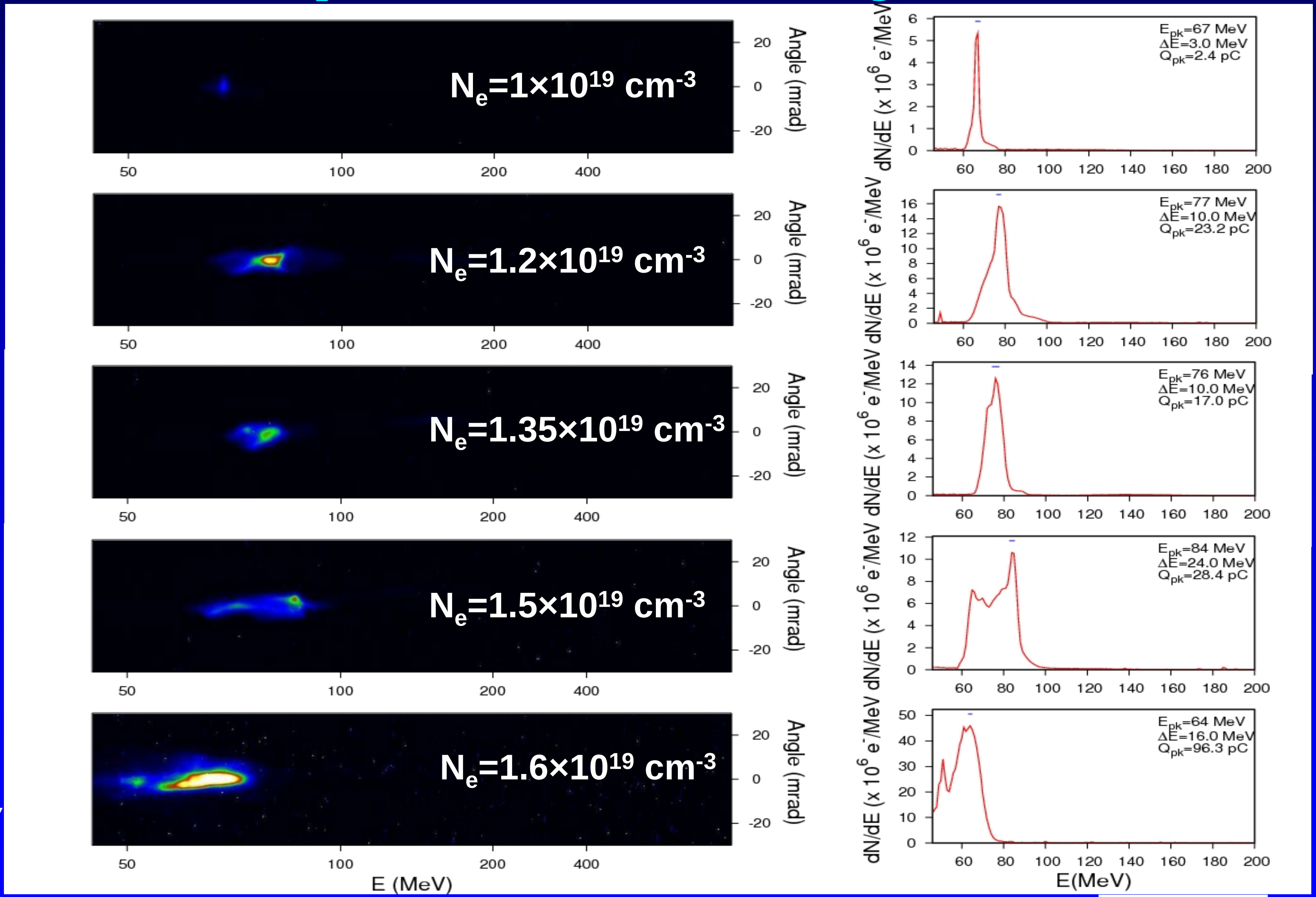

L O A

Tuning the charge with injection beam intensity a_1

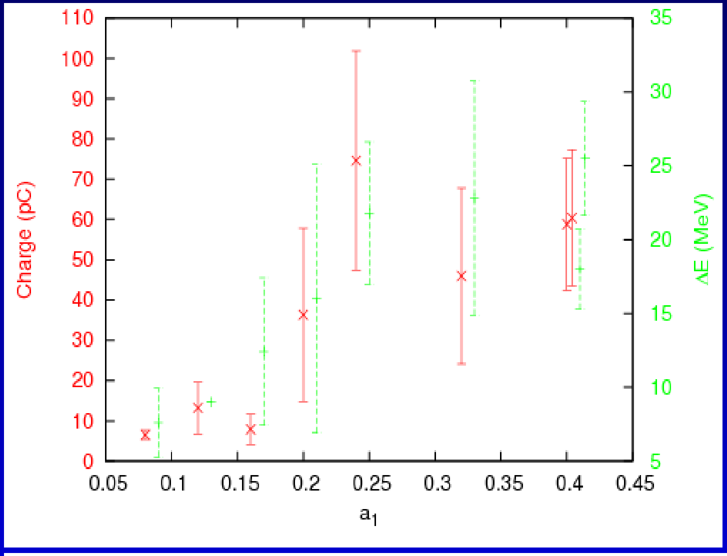

Charge from 60 pC to 5 pC

ΔE from 20 to 5 MeV

Energy stays similar

a_1=0.4

a_1=0.1

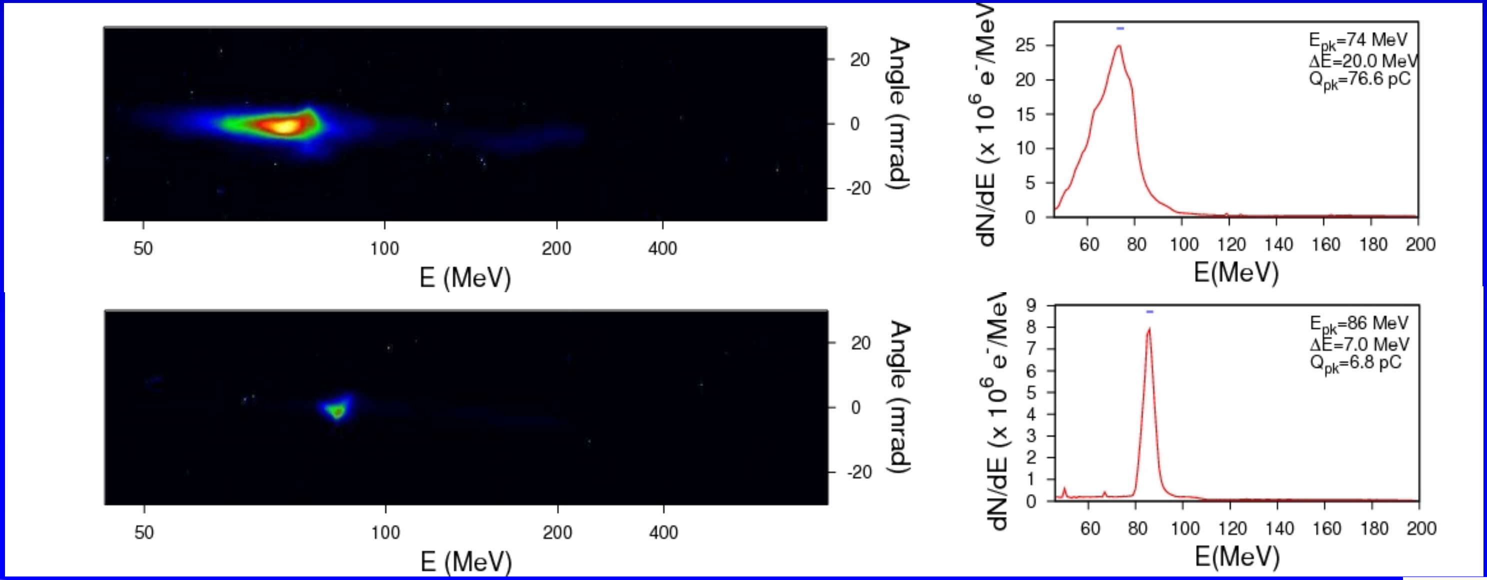

L O A

Collaboration with LLR* for resolving small energy spread beams

Gas jet

quadripoles

Permanent dipole

LANEX screens

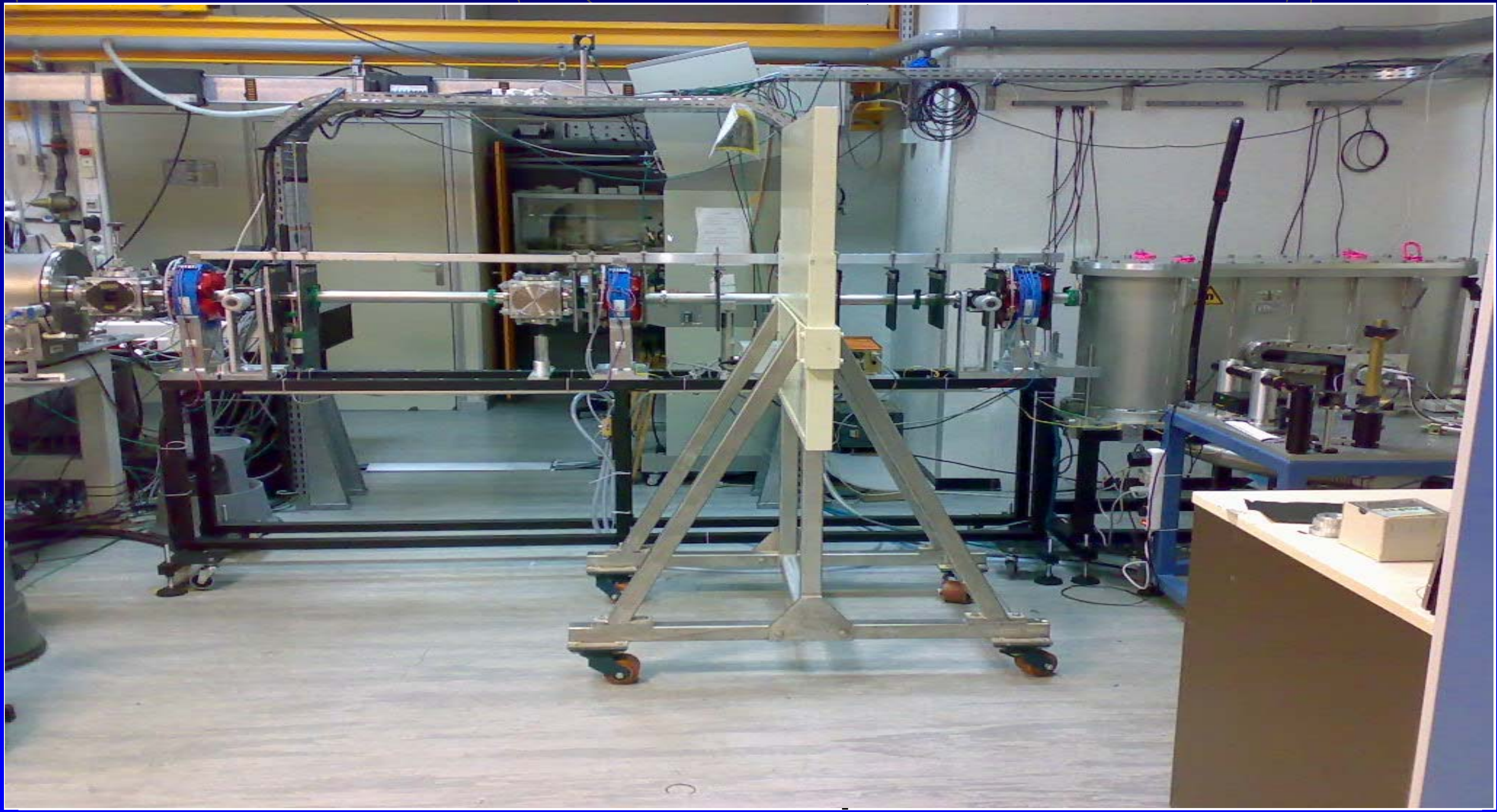

* A. Specka, H. Videau

L O A

ENSTA

POLYTECHNIQUE

1% energy spread beams

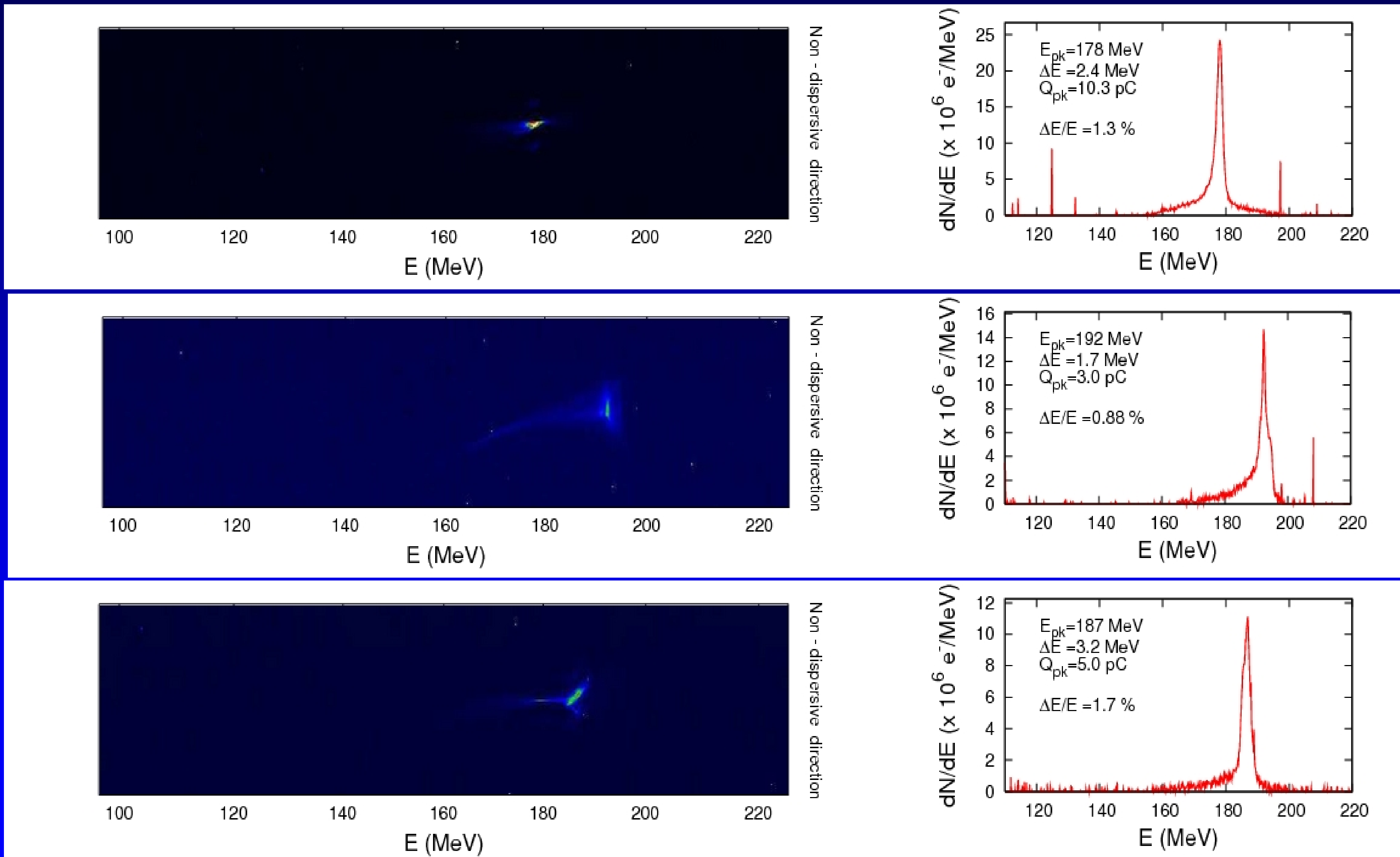

Conclusion

Two laser beams allows control of many e-beam parameters

- Good beam quality √
  - **Monoenergetic**, collimated beam √
  - δE/E down to 5 % , dE ~ 5-20 MeV, charge 10's pC √
- Beam is stable √
- Energy is tunable: 20-300 MeV √
- Charge is tunable: 1 to 100 pC √
- Energy spread is tunable: 5 to 20 % √
- Low energy spread beams at ΔE/E=1% √

WHAT'S NEXT ?

- Push energy limit (>1 GeV)
- Measure the bunch duration

(simulation and exp data indicates τ_{bunch}<10fs)

- Measure the emittance => EUCARD
- Increase injected charge: larger a_1 ?

L O A

LOA/CARE_PHIN : contribution 04-08

21 in refereed journals : 2 nature, 1 PRSTAB, 1 EuroPhys Lett, 1 PRL, etc..

50 Invited talks in International Conference

7 proceedings

Thanks to CARE the LOA group got several prizes :

Fresnel Prize to Jerome Faure
EPS PhD prize to Yannick Glinec
IEEE Prize to Victor Malka
La Recherche Magazine prize to V. Malka, J. Faure and E. Lefebvre

And ERC senior grant to V. Malka

Many thanks to the "accelerators" community for their supports and for hosting our approach in their program at a early, at a time where nothing (or quite) Was yet achieved.

Victor Malka

LOA

LOA/CARE_PHIN : List of publications in refereed journals 04-08

21 Direct observation of betatron oscillations in a laser-plasma electron accelerator
Y. Glinec, J. Faure, A. Lifschitz, J.M. Vieira, R.A. Fonseca, L. O Silva, V. Malka, Euro. Phys. Lett. 81, 64001 (2008).
20 Experiments and simulations of the colliding pulse injection of electrons in plasma wakefields
J. Faure, C. Rechatin, A. Lifschitz, X. Davoine, E. Lefebvre, V. Malka, IEEE transactions on plasma sceince, 36, 4 (2008).
19 Particle-in-Cell modelling of Laser-Plasma interaction using Fourier decomposition
A.F. Lifschitz, X. Davoine, E. Lefebvre, J. Faure, C. Rechatin, V. Malka, Journal of computational physics.
18 GeV monoenergetic electron beam with laser plasma accelerator
V. Malka, A. Lifschitz , J. Faure, Y. Glinec, International journal of modern physics B 21, (3-4), p277-286 (2007).
17 Controlled injection in laser plasma accelerator
J. Faure, C. Rechatin, A. Norlin, F. Burgy, A. Tafzi, J. P. Rousseau, V. Malka, Plasma Physics and Controlled Fusion 49 B395-B402 (2007).
16 Controlled injection and acceleration of electrons in plasma wakefields by colliding laser pulses
J. Faure, C. Rechatin, A. Norlin, A. F. Lifschitz, Y. Glinec, V. Malka, Nature (2006)
15 Staged concept of laser plasma acceleration toward multi GeV electrons beams
V. Malka, J. Faure, Y. Glinec, A. Lifschitz, to be published to PR -STA
14 Absolute calibration for a broadrange single shot electron spectrometer
Y. Glinec, J. Faure, A. Guemnie-Tafo, V. Malka, et al., RS 2006I.
13 Ultra short laser pulses and ultra short electron bunches generated in relativistic laser plasma interaction.
J. Faure, Y. Glinec, G. Gallot, and V. Malka, Phys. Plasmas 13, 056706 (2006).
12 Design of a compact GeV Laser Plasma Accelerator
V.Malka, A. F. Lifschitz, J. Faure, Y. Glinec, NIM A 561, p310-131 (2006)
11 Wakefield acceleration of low energy electron bunches in the weakly nonlinera regime
A. F. Lifschitz, J. Faure, Y. Glinec, V. Malka, NIM A 561, p314-319 (2006)
10 Proposed Scheme for Compact GeV Laser Plasma Accelerator
A. Lifschitz, J. Faure, Y. Glinec, P. Mora, and V. Malka, Laser and Particle Beams 24, 255-259 (2006)
9 Radiotherapy with laser-plasma accelerators: application of an experimental quasi-monoenergetic electron beam
Y. Glinec, J. Faure, T. Fuchs, H. Szymanowski, U. Oelfke, and V. Malka, Med. Phys. 33, (1) 155-162 (2006)
8 Laser-plasma accelerator: status and perspectives
V. Malka, J. Faure, Y. Glinec, A.F. Lifschitz, Royal Society Philosophical Transactions A, 364, 1840, 601-610 (2006)
7 Observation of laser pulse self-compression in nonlinear plasma waves
J. Faure, Y. Glinec, J. Santos, V. Malka, S. Kiselev, A. Pukhov, and T. Hosokai, Phys. Rev. Lett. 95, 205003 (2005).
6 Laser-plasma accelerators: A new tool for science and for society
V. Malka, J. Faure, Y. Glinec, and A.F. Lifschitz, Plasmas Physics and Controlled Fusion 47 (2005) B481-B490.
5 GeV Wakefield acceleration of low energy electron bunches using Petawatt lasers
A.F. Lifschitz, J. Faure, V. Malka, and P. Mora, Phys. of Plasmas 12, 0931404 (2005).
4 Generation of quasi-monoenergetic electron beams using ultrashort and ultraintense laser pulses
Y. Glinec, J. Faure, A. Pukhov, S. Gordiendko, S. Kiselev, V. Malka, Laser and Particle beams 23, 161-166 (2005).
3 Monoenergetic electron beam optimisation in the bubble regime
V. Malka, J. Faure, Y. Glinec, A. Pukhov, J.P. Rousseau, Phys. of Plasmas 12, 056702 (2005).
2 High-resolution -ray radiography produced by a laser-plasma driven electron source
Y. Glinec, J. Faure, L. Le Dain, et al., Phys. Rev. Lett.94 (2005).
1 A laser-plasma accelerator producing monoenergetic electron beams
J. Faure, Y. Glinec, A. Pukhov, et al., Nature 431, 541, 30 septembre (2004).

L O A